Available online at www.sciencedirect.com
SCIENCE DIRECT®
Journal of Nuclear Materials 337–339 (2005) 134–138
journal of nuclear materials
www.elsevier.com/locate/jnucmat

Measurements of carbon, deuterium and boron deposition in DIII-D

W.R. Wampler [a,*], S.L. Allen [b], A.G. McLean [c], W.P. West [d]

[a] Sandia National Laboratories, P.O. Box 5800, Albuquerque, NM 87185-1056, USA
[b] Lawrence Livermore National Laborabory, Livermore, CA 94550, USA
[c] University of Toronto Insitute for Aerospace Studies, Toronto, Canada MH3 5T6
[d] General Atomics, San Diego, CA 92186-5608, USA

Abstract

An experiment was recently conducted in DIII-D in which ^{13}C methane ($^{13}CH_4$) was injected from the upper divertor plenum into 22 identical lower single null divertor L-mode plasmas. Twenty-nine graphite tiles were subsequently removed and analyzed to determine the spatial distribution of ^{13}C deposited on the main chamber wall and divertor. ^{13}C coverage was mapped by ion beam analysis using the $^{13}C(^3He,p)^{15}N$ nuclear reaction. This technique also measures deuterium, boron and ^{12}C content in the near-surface region of the tiles. The measurements show the ^{13}C is deposited mainly at the inner divertor.

PACS: 52.40.Hf; 52.55.Fa; 28.52.Fa
Keywords: DIII-D; $^{13}CH_4$ injection; Nuclear reaction analysis; Erosion/deposition; Impurity transport

1. Introduction

Codeposition of tritium with carbon can potentially lead to large inventories of retained tritium in a fusion reactor [1]. In tokamaks with carbon walls, hydrocarbons from chemical erosion at the wall dissociate in the plasma edge and redeposit back onto plasma facing surfaces. The location and form of this redeposited carbon affects tritium retention and strategies for its mitigation. Models are being developed to simulate and predict erosion, transport and deposition of carbon in tokamaks [2,3] and experiments are needed to test the models. Such an experiment was recently conducted in DIII-D in which $^{13}CH_4$ was injected from the upper divertor plenum into lower single null divertor L-mode deuterium fuelled plasmas, as illustrated in Fig. 1 [4]. This plasma geometry and location of injection far from the divertor, were chosen to simulate methane originating from plasma interactions with the main chamber wall. A set of graphite tiles was subsequently removed and analyzed to determine the spatial distribution of ^{13}C deposition on the main chamber wall and divertor. ^{13}C coverage was mapped by ion beam analysis using $^{13}C(^3He,p)^{15}N$ nuclear reaction analysis. This technique also measures deuterium, boron and ^{12}C content in the near-surface region of the tiles. This paper describes the ion beam analysis method used and presents the results of the measurements. The distribution of ^{13}C shows the pattern of carbon deposition with the well-defined plasma

* Corresponding author. Tel.: +1 505 844 4114; fax: +1 505 844 7775.
E-mail address: wrwampl@sandia.gov (W.R. Wampler).

0022-3115/$ - see front matter © 2004 Elsevier B.V. All rights reserved.
doi:10.1016/j.jnucmat.2004.10.124

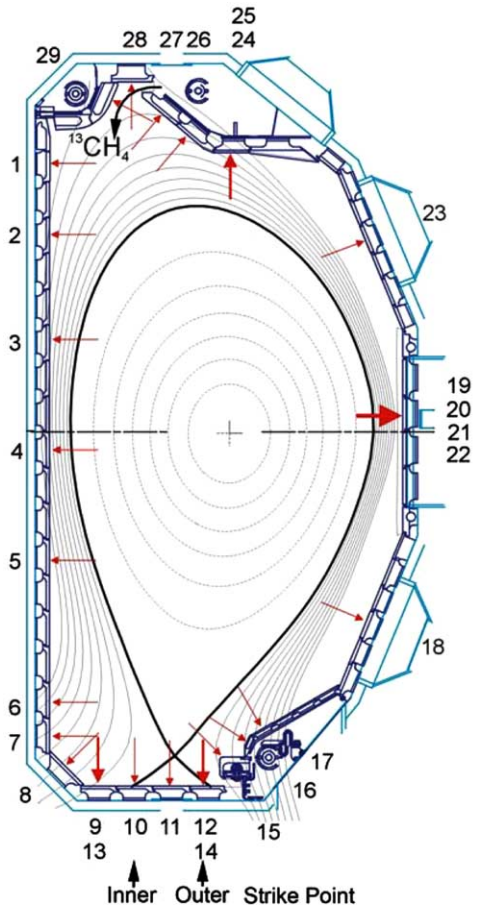

Fig. 1. Illustration of the plasma configuration and location of $^{13}CH_4$ injection. Red arrows and numbers indicate tiles analyzed. Heavy red arrows indicate tiles from multiple toroidal angles. The lines indicate magnetic field contours (dotted) and the last closed flux surface (heavy). Radii of the inner and outer wall at the midplane are 1.01 and 2.38 m respectively from the center of the machine (For interpretation of the refrences in colour in this figure legend, the reader is referred to the web version of this article).

conditions during the $^{13}CH_4$ injection, while the distributions of boron and deuterium indicate the wall composition resulting from erosion and deposition during prior exposure to various plasmas and wall conditioning procedures. The measurements show the ^{13}C is deposited primarily at the inner divertor.

2. Experimental methods

$^{13}CH_4$ was injected from a distributed gas system located in the upper divertor plenum providing a high degree of toroidal symmetry to the $^{13}CH_4$ flow into the plasma. The $^{13}CH_4$ was injected for 3 s intervals during constant plasma conditions, at a rate chosen to be as high as possible without significantly perturbing the plasma conditions [4]. Plasma conditions are described in references [4,5]. Tiles were near room temperature except at the strike point where the temperature rose during the plasma exposure but remained below 100 °C during the low power L-mode plasmas used in this experiment [6]. In order to obtain a sufficient total quantity of ^{13}C for measurements of deposition, the $^{13}CH_4$ injection was repeated for 22 consecutive identical plasmas, for a total of 314 Torr-liters or 1.00×10^{22} atoms of injected ^{13}C. The $^{13}CH_4$ injection was done on the last day of the experimental campaign, and no baking or cleaning were performed afterwards. At the beginning of the subsequent machine vent, 29 carbon tiles were removed for analysis. These tiles were located both in the divertor and main chamber, as illustrated in Fig. 1. The tile set included 23 tiles within ±10° of the same toroidal angle, plus 6 from other toroidal angles to check toroidal symmetry.

^{13}C coverage on the tiles was measured by ion beam analysis at Sandia National Laboratories, using a large chamber capable of analyzing whole tiles. An analysis beam of 2.5 MeV ^3He was directed onto the tiles, and energy spectra of charged particles from resulting nuclear reactions were recorded. Measurement of ^{13}C coverage required a specialized detector geometry optimized for this purpose. A large diameter annular silicon surface barrier detector 3 cm from the target was used to obtain a large solid angle without excessively broadening the energy resolution due to the range of scattering angles subtended. A large depletion depth of 1500 μm is necessary to stop the energetic protons.

Fig. 2 shows spectra of protons from the $^{13}C(^3He,p)^{15}N$ reaction for a graphite sample, a thin film ^{13}C reference sample, and two of the tiles from DIII-D. The ^{13}C thin film reference has a narrow peak at 10.6 MeV. This peak is also present for graphite because it contains 1.1% natural abundance of ^{13}C. The broadening of the peak for graphite results mainly from the kinematics of the reaction and the fact that the ^3He loses energy as it penetrates into the target. The lower energy ^3He at greater depths yields lower energy protons. The detector must therefore have good energy (and thus depth) resolution to distinguish ^{13}C deposited on the tile surface from natural ^{13}C in the graphite. The energy resolution indicated by the width of the ^{13}C reference peak in Fig. 2, corresponds to a depth resolution for the ^{13}C analysis of about 0.6 μm.

Nuclear reactions with other light isotopes present on the tiles produce energetic particles at many other energies. Thin film references were used to link peaks in the energy spectra to isotopes and check for overlapping peaks. Yields from proton peaks at 11.4, 9.2 and 3.2 MeV were used to determine near-surface content of deuterium, boron and ^{12}C respectively.

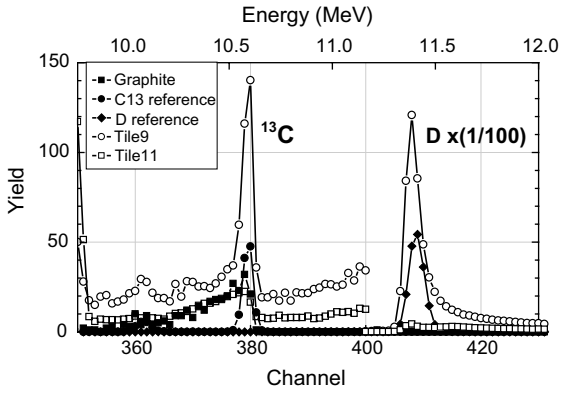

Fig. 2. Energy spectra of protons from the $^{13}C(^3He,p)^{15}N$ nuclear reaction for a graphite sample, a thin film ^{13}C reference sample, a thin film deuterium reference, and two of the tiles from DIII-D. The ^{13}C reference spectrum has been scaled to indicate the yield from 10^{17} atoms/cm^2. The deuterium reference spectrum has been scaled to indicate the yield from 10^{18} atoms/cm^2. Above channel 400 data have been scaled down by a factor of 100 so that peaks from ^{13}C and deuterium can both be clearly seen.

Coverage, or areal density, of ^{13}C deposited on the tiles was determined from the yield of 10.6 MeV protons summed over the region of the peak in the ^{13}C thin film reference spectrum (channels 378 to 381 in Fig. 2). From this yield a background, consisting of two components, was subtracted. The first background component can be seen as an offset just above the ^{13}C peak in the tile spectra in Fig. 2. This background is probably from higher energy protons which have lost some of their energy in a scattering event before entering the detector. It is expected to have weak energy dependence and is taken to be the yield just above the ^{13}C peak. The second background component is due to the natural abundance of ^{13}C in graphite. For a graphite substrate this would be the yield from the graphite reference summed over the region of the reference ^{13}C peak. For graphite this background component corresponds to the yield from 0.7×10^{17} atoms/cm^2 of ^{13}C on the surface, or to the ^{13}C naturally occurring in 0.6 μm of graphite. However, due to the boronization done in DIII-D [7], the first micron of the tiles contains boron in addition to carbon, so the background from this second component has been weighted according to the fraction of carbon C/(C + B). The fractions of carbon and boron near the surface of the tiles were determined using proton peaks at 3.2 and 9.2 MeV for ^{12}C and boron respectively (not shown in Fig. 1), and by comparing the yields from these peaks for the DIII-D tiles with yields from graphite and B_4C reference samples.

The areal density of ^{13}C deposited onto the tile surfaces was thus determined from the measured yield of 10.6 MeV protons, remaining after background subtraction, with a conversion factor determined from the yield from a reference sample (a thin film of isotopically pure ^{13}C on a silicon substrate). The areal density of ^{13}C on the reference was $(22\pm2)\times10^{17}$ atoms/cm^2, determined by Rutherford backscattering using 1.5 MeV ^4He. The standard deviation in measurements of ^{13}C on the tiles, due to counting statistics, is about 0.1×10^{17} atoms/cm^2. The total uncertainty in the measurements of ^{13}C coverage is estimated to be $\pm0.2\times10^{17}$ atoms/cm^2. Thus the lowest detectable ^{13}C deposition is about 0.2×10^{17} atoms/cm^2. For comparison, the injected quantity of ^{13}C distributed uniformly over the wall of DIII-D would give a coverage of about 0.1×10^{17} atoms/cm^2. Negative values of ^{13}C deposition plotted in Fig. 3 are due to inaccuracies in subtraction of background, and are within the estimated uncertainty of the measurement.

The areal density of deuterium in the DIII-D tiles was determined from the yield of protons from the $^2H(^3He,^1H)^4He$ nuclear reaction, over an energy range corresponding to deuterium within 2 μm of the surface. The deuterium analysis was quantified using a reference consisting of a 0.5 μm film of ErD_2, which contained $(26.5\pm1.3)\times10^{17}$ D/cm^2 as determined by thermal desorption gas analysis on sister samples [8]. The energy spectra of these protons can be transformed into the deuterium concentration versus depth extending to a maximum depth of 7 μm, using known stopping power and nuclear reaction cross section and kinematics.

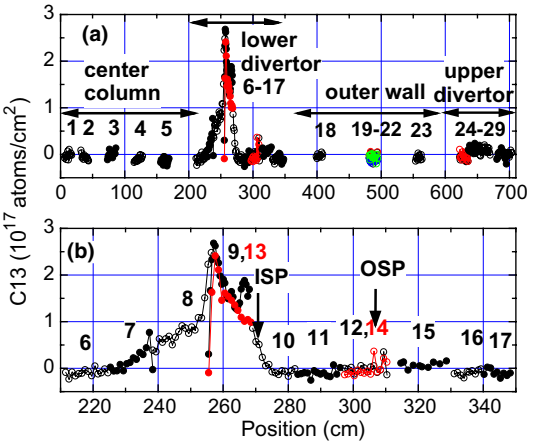

Fig. 3. The symbols show measured ^{13}C deposition on the tiles. The horizontal coordinate is the distance in the counterclockwise poloidal direction along the tile surfaces from the top of the center column as shown in Fig. 1. The top panel (a) shows data from all 29 tiles. The bottom panel (b) shows an expanded view of data from the lower divertor. The arrows indicate the location of the inner strike point (ISP) and outer strike point (OSP). Numbers indicate tiles as identified in Fig. 1. Different colors indicate tiles from different toroidal angles.

3. Results

Measurements were made along scans in the poloidal direction through the center, and near the edges of each tile. Additional poloidal scans were done on some tiles. Measurements were made from edge to edge at 1 cm intervals for most scans. In nearly all cases the ^{13}C distribution was similar for the various scans on a given tile, and for tiles from the same poloidal position but at different toroidal angles, indicating that the ^{13}C deposition was fairly symmetric toroidally.

Fig. 3 shows the measured ^{13}C deposition on the tiles. The plot shows the average value from the various scans on each tile. The horizontal coordinate is the distance in the poloidal direction along the tile surfaces counterclockwise from the top of the center column as shown in Fig. 1. The top panel shows data from all 29 tiles. The bottom panel shows an expanded view of data from the lower divertor. The location of the inner and outer strike points during the $^{13}CH_4$ injection are indicated by arrows at positions 270.5 and 306.7 cm, corresponding to DIII-D major radii of 129 and 165.5 cm respectively. ^{13}C deposition is observed mainly on tiles 7, 8, 9, 10 and 13 at the inner divertor. Little or no ^{13}C deposition was found at the outer divertor or outside the divertor region. In particular, ^{13}C deposition was below the limit of detection (0.2×10^{17} atoms/cm^2) on tiles near the region of $^{13}CH_4$ injection. The low ^{13}C coverage on the left edge of tiles 9 and 13 is due to shadowing by overlapping adjacent tiles. By integrating the data in Fig. 3 the total quantity of ^{13}C deposited onto the plasma-facing surfaces of the tiles is found to be 0.30×10^{22} atoms, assuming toroidally symmetric deposition. This is only 30% of the quantity injected. Some of the remaining 70% may have been deposited over large areas below the detection limit of this measurement, and some may have been pumped away during helium glow discharge conditioning (He GDC), which occurred for 5 min between plasmas. Residual gas analysis of exhaust gas during He GDC, showed an increase in mass 21 (corresponding to $^{13}CD_4$) by an order of magnitude after injecting plasmas with $^{13}CH_4$. Though not quantitative, the RGA data shows that some of the deposited ^{13}C was removed as hydrocarbons during subsequent He GDC. A study conducted in JET, in which $^{13}CH_4$ was injected from one toroidal location at the top of the main plasma chamber, also found deposition of ^{13}C on the inner divertor but not on the outer divertor [9].

Fig. 4 shows plots of the distribution of deuterium content within about 2 μm of the surface. The highest deuterium coverage is at the inner divertor, indicating deuterium accumulation by codeposition in this region. The relatively low deuterium coverage in the private flux region (tile 11) and the center column indicates that these are not regions of high net codeposition. Fig. 5 shows the distribution of the fraction of boron

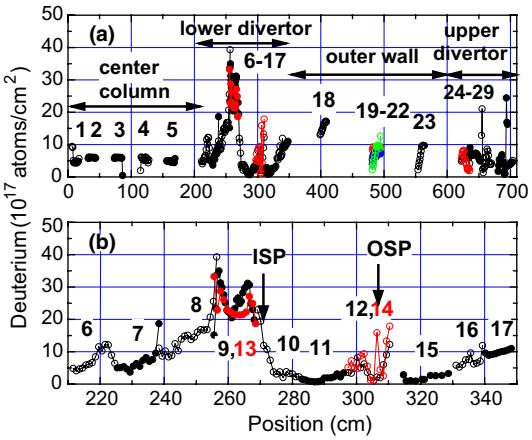

Fig. 4. A plot similar to Fig. 3 but showing deuterium content in the first 2 μm of the tiles.

B/(B + C) within about 1 micron of the surface. Thin (~0.1 μm) coatings of boron are periodically applied by plasma assisted chemical vapor deposition of diborane to condition the wall [7]. Subsequent plasma operation may (1) remove the boron, exposing the underlying graphite in regions of high net erosion, (2) cover the boron with carbon and deuterium in regions of high net codeposition, or (3) leave boron at the surface in regions of little or no erosion or deposition. Comparing Figs. 4 and 5 we see that the inner divertor (tiles 9 and 13) has relatively low boron, i.e. high carbon, and high deuterium, consistent with net codeposition of carbon and deuterium in this region. The outer divertor (tiles 15, 16 and 17) and center column (tiles 1 through 5) have low boron and low deuterium consistent with net erosion. Tiles (18, 19 and 23) on the outer wall have high boron content and low deuterium content, indicating this is a region of little or no net erosion or deposition.

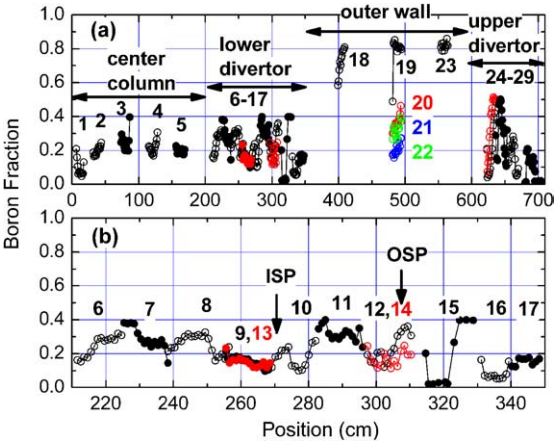

Fig. 5. A plot similar to Figs. 3 and 4 but showing the fraction of boron B/(B + C) near the surface.

Tiles (20, 21 and 22) from the bumper limiters had lower boron and low deuterium indicating higher erosion than the outer wall tiles, presumably due to their closer contact with the plasma. The toroidal asymmetry in boron fraction on tiles 20–22 might result from asymmetric boron deposition during boronization, or from asymmetric erosion.

4. Conclusions

Ion beam analysis of tiles from DIII-D provides a clearer picture of carbon erosion, transport in the SOL and deposition. Analysis of deuterium, carbon and boron content of the near-surface region of the tiles shows regions of erosion and deposition. High deuterium and low boron coverage at the inner divertor show this is the region of highest net codeposition, consistent with the result from the $^{13}CH_4$ injection experiment. The outer divertor and center column have low boron and low deuterium indicating net erosion. High boron content and low deuterium content on the outer wall tiles indicate this is a region of little or no net erosion or deposition. The relatively low deuterium coverage in the private flux region indicates this is not a region of high net codeposition.

Injection of $^{13}CH_4$ from the upper divertor plenum into lower single null L-mode plasmas results in heaviest deposition of ^{13}C at the inner divertor, with little or no deposition observed elsewhere. Prompt local deposition of ^{13}C near the region of injection, via neutral dissociation fragments is below the detection limit. Carbon from methane entering the plasma in the main chamber is ionized in the scrape-off layer and transported preferentially towards the inner divertor where it is deposited onto surfaces intersecting field lines. Measured ^{13}C deposition was about 30% of the injected amount. The remaining 70% may have been pumped away during helium glow discharge conditioning between plasmas, or deposited over large areas below the detection limit of this measurement. Details of the location and shape of deposited ^{13}C provide a critical test of plasma boundary models [2,3], which are needed for the design of future fusion devices.

Acknowledgments

Sandia is a multiprogram laboratory operated by Sandia Corporation, a Lockheed Martin Company, for the US Department of Energy. This work was supported by the US Department of Energy under Contract Nos. W-7405-ENG-48, DE-FC02-04ER54698 and DE-AC04-95ER85000.

References

[1] G. Federici, C.H. Skinner, J.N. Brooks, et al., Nucl. Fusion 41 (2001) 1967.
[2] J.D. Elder, P.C. Stangeby, D.G. Whyte, et al., these Proceedings, doi:10.1016/j.jnucmat.2004.10.138.
[3] A.G. McLean, J.D. Elder, P.C. Stangeby, et al., these Proceedings, doi:10.1016/j.jnucmat.2004.10.130.
[4] S.L. Allen, A.G. McLean, W.R. Wampler, et al., these Proceedings, doi:10.1016/j.jnucmat.2004.09.066.
[5] D.L. Rudakov et al., these Proceedings, doi:10.1016/j.jnucmat.2004.10.094.
[6] J.G. Watkins, C.J. Lasnier, D.G. Whyte, et al., Rev. Sci. Instrum. 74 (2003) 1574.
[7] K.L. Holtrop, G.L. Jackson, A.G. Kellman, et al., J. Vacuum Sci. Technol. A 15 (1997) 678.
[8] J.C. Banks, J.F. Browning, W.R. Wampler, et al., Nucl. Instrum. and Meth. B 219&220 (2004) 444.
[9] J. Likonen, S. Lehto, J.P. Coad, et al., Fusion Eng. Des. 66–68 (2003) 219.